Delitpyrones: *α*-Pyrone Derivatives from a Freshwater *Delitschia* sp.

By: José Rivera-Chávez, Tamam El-Elimat, Jacklyn M. Gallagher, Tyler N. Graf, Jacques Fournier, Gati K. Panigrahi, Gagan Deep, Rick L. Bunch, Huzefa A. Raja, and Nicholas H. Oberlies

Abstract:

In research focused on the discovery of new chemical diversity from freshwater fungi, a peak library was built and evaluated against a prostate cancer cell line, E006AA-hT, which was derived from an African American, as this population is disproportionately affected by prostate cancer. The chemical study of the bioactive sample accessioned as G858 (*Delitschia* sp.) led to the isolation of eight new *α*-pyrone derivatives (**1**–**7**, and **11**), as well as the new 3S*,4S*-7-ethyl-4,8-dihydroxy-3,6-dimethoxy-3,4-dihydronaphthalen-1(*2H*)-one (**15**). In addition, the known compounds 5-(3-*S*-hydroxybutyl)-4-methoxy-6-methyl-2*H*-pyran-2-one (**8**), 5-(3-oxobutyl)-4-methoxy-6-methyl-2*H*-pyran-2-one (**9**), pyrenocine I (**10**), 5-butyl-6-(hydroxymethyl)-4-methoxy-2*H*-pyran-2-one (**12**), sporidesmin A (**13**), 6-ethyl-2,7-dimethoxyjuglone (**14**), artrichitin (**16**), and lipopeptide 15G256*ε* (**17**) were also obtained. The structures of the new compounds were elucidated using a set of spectroscopic (NMR) and spectrometric (HRMS) methods. The absolute configuration of the most abundant member of each subclass of compounds was assigned through a modified Mosher's ester method. For **15**, the relative configuration was assigned based on analysis of ^3J values. Compounds **1, 2, 5**–**14, 16**, and **17** were evaluated against the cancer cell line E006AA-hT under hypoxic conditions, where compound **13** inhibited cell proliferation at a concentration of 2.5 µM.

Article:

Introduction

The fungal kingdom, estimated at 2.2–3.8 million species, with just 3 to 8% identified (120 000) [1], is the second most diverse on the planet [2]. Among those, the freshwater ascomycetes are underinvestigated, with only about 675 species described [3]. This diverse ecological group

relies upon freshwater for the whole or part of their life cycle [3],[4] and includes any species growing on substrates that are aquatic or semiaquatic [4]. Freshwater fungi play an important role in the degradation of organic materials [5]. Chemically, the ability of freshwater ascomycetes to produce bioactive metabolites merits investigation, as less than 250 metabolites have been described [6]. Thus, to contribute to the expansion of the chemical space of secondary metabolites from this ecological niche, our team has started a systematic study of bioactive compounds from freshwater ascomycetes [7]. Recent examples include five acetophenone derivatives [8] and 14 resorcylic acid lactones with cytotoxic activity [9], as well as isochromenones, isobenzofuranones, and tetrahydronaphthalenes [10].

According to Index Fungorum (http://www.indexfungorum.org/names/names.asp) and the Dictionary of Fungi [11], the genus *Delitschia* Auersw. (Delitschiaceae) comprises coprophilous and saprobic taxa with around 83 species; another resource (Genera of Ascomycota) lists a more conservative 52 species. Despite the diversity in this genus, only a handful have been investigated for bioactive secondary metabolites. Interestingly, the few chemical studies conducted of this genus have led to the isolation of compounds with new scaffolds, such as delitschiapyrone A [12], an α-pyrone-naphthalenone adduct, and a fimetarone derivative [13].

In the USA, African American men have the highest risk of both developing and dying of prostate cancer, relative to Caucasians [14],[15], and there are many social, economic, and biological factors that contribute to this health disparity [15]. Hence, with the goals of understanding the biology and ameliorating this disease, we have initiated a project focused on the discovery of research tools and drug leads for the treatment of prostate cancer in African Americans. Hypoxia (low oxygen conditions) in prostate tumors is an early event associated with an aggressive phenotype. Hypoxic conditions in the tumor microenvironment promote genetic, metabolic, and proteomic changes, which lead to increased glycolysis, angiogenesis, survival, stemness, invasiveness, and selection of resistant clones [16]. Levels of hypoxia in prostate tumors, and expression of hypoxia-related biomarkers (e.g., hypoxia-inducible factor HIF1α and HIF2α), are associated with poor prognosis and are the major reasons for treatment failure and disease relapse [16]. Therefore, we assessed the effect of potential drugs against African American prostate cancer cells under hypoxic conditions.

In this context, a study of the aquatic fungus *Delitschia* sp. (strain G858) led to the isolation and characterization of eight new structurally related α-pyrone derivatives (**1**–**7**, and **11**), as well as one new dihydronaphthalenone (**15**), along with eight known fungal metabolites (**8**–**10, 12**–**14, 16**, and **17**). The cytotoxic activities of compounds **1, 2, 5**–**14, 16**, and **17** were evaluated against the E006AA-hT cell line, where compound **13** showed promising bioactivity.

Results and Discussion

A library of 64 freshwater fungal isolates from diverse habitats (**Fig. 58S**, Supporting Information), arrayed across 320 peaks, was assembled using an 8-step procedure. Starting with a mature fungal culture, the sample was first extracted and then fractionated into four peaks. These samples were used to generate mother plates (10 mg/mL), daughter plates (5 mg/mL), and granddaughter plates (5 µg/well); each plate represented 16 fungi over 80 wells (16 extracts plus 4 fractions from each). The plates were evaluated in a panel of bioassays, and hits were

prioritized and dereplicated [17],[18]. The parent samples of active fractions were then used for isolation and elucidation of the hits, and this included fungal culture scale-up, when needed. Finally, pure compounds were evaluated for biological activities ([Fig. 1]).
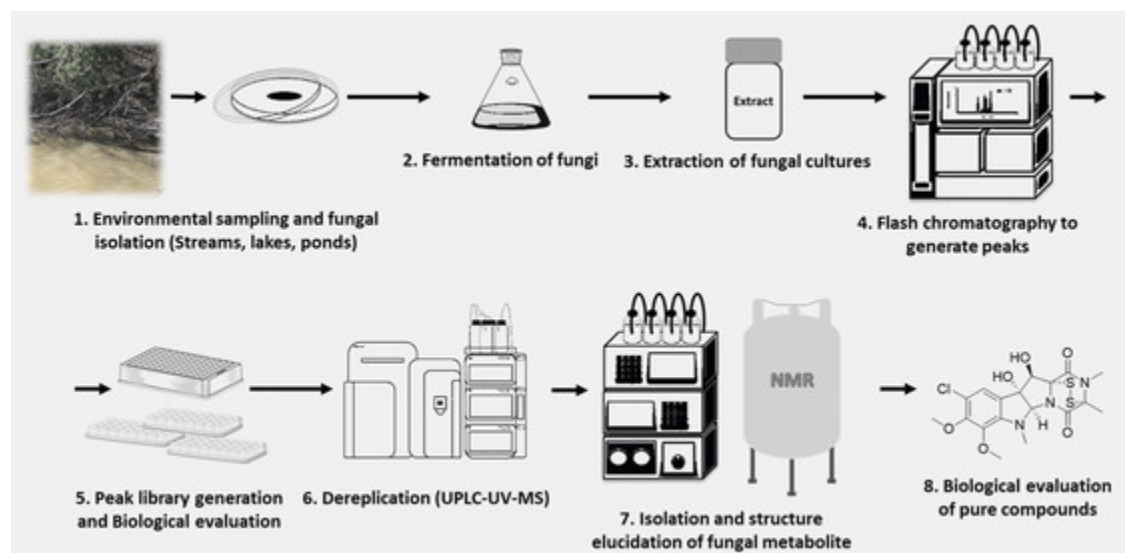

Figure 1. Strategy for uncovering new natural products from fungal peak libraries. The procedure starts with the sampling and isolation of axenic fungal strains, followed by fermentation, extraction, and fractionation into peaks. The peaks are used to generate mother plates, daughter plates, and granddaughter plates; each plate represents 16 fungal isolates over 80 wells (16 extracts plus 4 fractions from each). The plates are then evaluated in a panel of bioassays, and hits are prioritized and dereplicated. The parent samples of active fractions are used for isolation and elucidation of hits. Finally, pure compounds are evaluated for biological activities.

The library was tested against an African American prostate cancer cell line (E006AA-hT) under hypoxic conditions (1% O_2), where cancer cells are more drug resistant [19],[20]. Promising bioactivity was observed with peaks derived from strain G858 (20% viability when tested at a concentration of 2 µg/mL) (**Fig. 1S**, columns 1 and 3, Supporting Information). These samples displayed an HPLC-UV profile that indicated a series of related analogues (Supporting Information), which could not be identified using the dereplication protocols [17],[18].

A large-scale culture of G858 (*Delitschia* sp.) was grown on rice and extracted using protocols described previously [21]. The resultant extract was partitioned using organic solvents and fractionated using flash chromatography, yielding nine fractions. These were purified further using preparative and semipreparative HPLC to yield nine new natural products (**1**−**7, 11**, and **15**), along with the known compounds 5-(3-S-hydroxybutyl)-4-methoxy-6-methyl-2H-pyran-2-one (**8**) [22], 5-(3-oxobutyl)-4-methoxy-6-methyl-2*H*-pyran-2-one (**9**) [23], pyrenocine I (**10**) [24], 5-butyl-6-(hydroxymethyl)-4-methoxy-2*H*-pyran-2-one (**12**) [23], sporidesmin A (**13**) [25], 6-ethyl-2,7-dimethoxyjuglone (**14**) [12],[26], artrichitin (**16**) [27], and lipopeptide 15G256ε (**17**) [28] ([Fig. 2]). The structures of the isolates were established using spectroscopic and spectrometric data, which for all known compounds compared favorably to the literature. The absolute configuration of an illustrative member of each subclass was assigned through a modified Mosher's ester method [29].
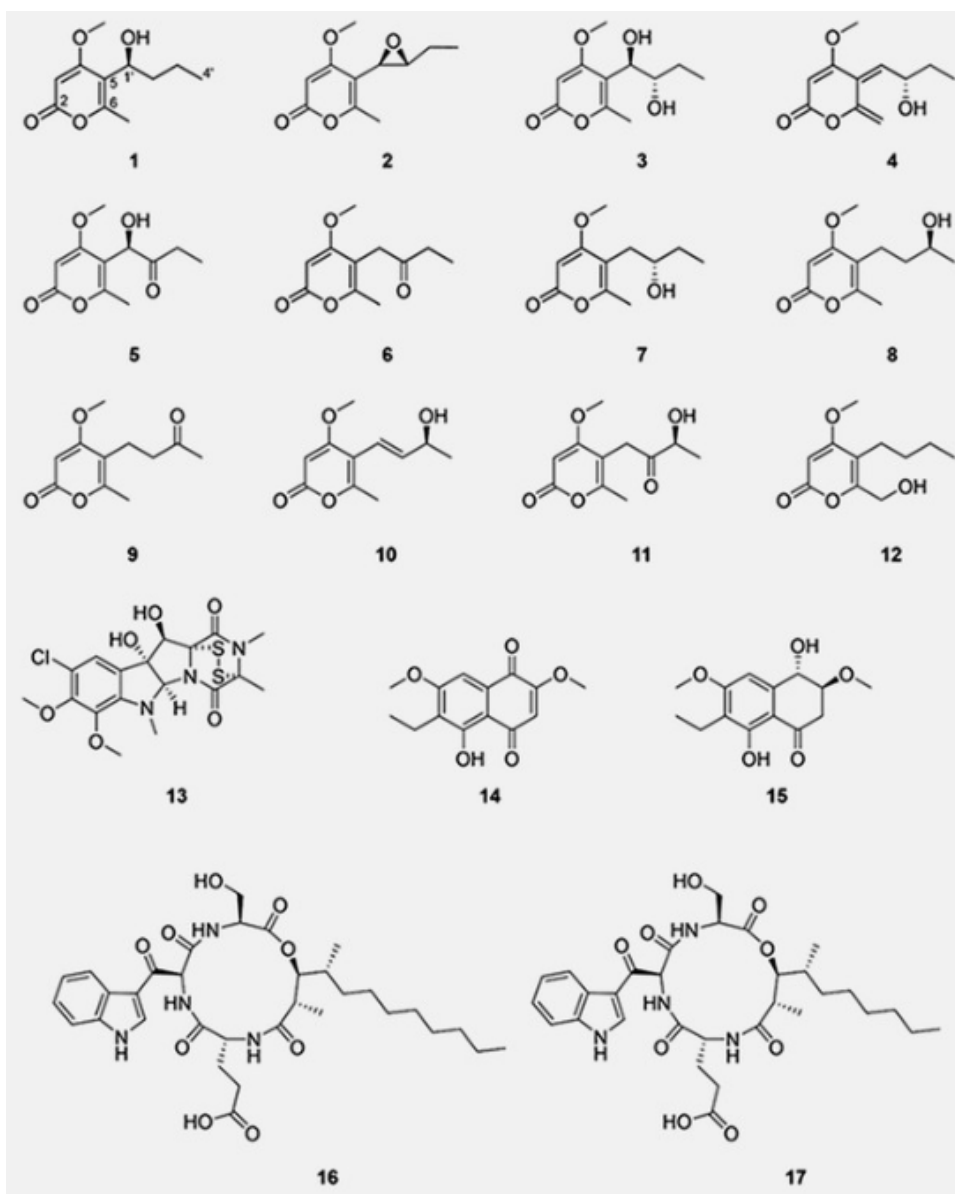
Figure 2. Structures of compounds **1–17**.

Compound **1** was isolated as a colorless solid, and its molecular formula was $C_{11}H_{16}O_4$ on the basis of the HRESIMS data (m/z 213.1125), indicating an index of hydrogen deficiency of four. The ^1H- and ^{13}C-NMR spectra ([Tables 1] and [2], **Figs. 5S** and **6S**, Supporting Information) in combination with HSQC data showed signals attributed to one olefinic proton (δ_H/δ_C 5.49/89.1), one methoxy group (δ_H/δ_C 3.86/56.3), one –OH (δ_H 2.44), two CH_2 (δ_H/δ_C 1.64/1.86/39.4; δ_H/δ_C 1.28/1.42/19.5), and two CH_3 groups (δ_H/δ_C 0.93/14.0; δ_H/δ_C 2.29/17.9), as well as four quaternary carbons, including three olefinic (δ_C 170.6, 113.2, and 159.1) and one carbonyl (δ_C 164.0), attributed to an α,β unsaturated lactone. In general, these data showed notable similarity to that of (R)-5-(1-hydroxybutyl)-4-methoxy-6-methyl-2H-pyran-2-one, an α-pyrone derivative isolated from *Alternaria phragmospora* [23]. In our study, the absolute configuration at C-1′ in **1** was established as *S* by comparison of its specific rotation ($[\alpha]_D^{27} = -15$) with that reported for its enantiomer (1′R)-

2′,3′-dihydropyrenocine C ($[\alpha]_D{}^{27}$ = + 15.7) [12], and based on the outcomes obtained after applying a modified Mosher's method ([Fig. 3]) [29]. Thus, compound **1** was identified as (1′*S*)-2′,3′-dihydropyrenocine C, and assigned the trivial name delitpyrone A (**1**).

Table 1. ^{1}H-NMR data for compounds **1−3, 5−7**, and **11**.

Position	δ_H, multiplicity (*J* = Hz)						
	1	**2**	**3**	**5**	**6**	**7**	**11**
3	5.49, *s*	5.45, *s*	5.54, *s*	5.48, *s*	5.46, *s*	5.58, *s*	5.47, *s*
1′	4.63, *q* (6.5)	3.71, *d* (4.0)	5.15, *d* (6.2)	4.98, *d* (3.5)	3.42, *s*	2.41, *dd* (14.1, 8.6) 2.58, *dd* (14.1, 4.2)	3.48, *d* (17.9); 3.55, *d* (17.9)
2′	1.64, *ddt* (13.5, 10.2, 6.1) 1.86, *dddd* (13.4, 10.1, 8.0, 5.3)	3.10, *ddd* (6.9, 5.2, 4.1)	4.52, *q* (6.2)			3.55, *tt* (8.5, 4.4)	
3′	1.28, *m*; 1.42, *m*	1.25, *dp* (14.4, 7.3) 1.35, *m*	1.77, *m* 1.86, *dp* (14.7, 7.4)	2.35, *q* (7.5); 2.35, *qd* (7.5, 0.5)	2.50, *q* (7.3)	1.46, *m*; 1.53, *m*	4.38, *dq* (6.9, 5.0)
4′	0.93, *t* (7.4)	0.99, *t* (7.5)	1.06, *t* (7.4)	1.11, *t* (7.3)	1.09, *t* (7.3)	0.98, *t* (7.4)	1.47, *d* (7.1)
4-OCH$_3$	3.86, *s*	3.82, *s*	3.89, *s*	3.78, *s*	3.78, *s*	3.88, *s*	3.77, *s*
6-CH$_3$	2.29, *s*	2.34, *s*	2.34, *s*	2.33, *s*	2.17, *s*	2.28, *s*	2.19, *s*
1′-OH	2.44, *d* (7.7)			4.02, *d* (3.7)			
3′-OH							3.28, *d* (5.0)

For solvents and magnetic field used for each compound, see the Materials and Methods section

Table 2. ^{13}C-NMR data for compounds **1−3, 5−7,** and **11**.

Position	δ_C, type													
	1		**2**		**3**		**5**		**6**		**7**		**11**	
2	164.0	C	164.3	C	162.5	C	163.3	C	164.3	C	167.4	C	169.5	C
3	89.1	CH	87.6	CH	89.4	CH	88.6	CH	88.0	CH	88.3	CH	88.2	CH
4	170.6	C	170.2	C	169.2	C	169.2	C	170.0	C	173.4	C	164.0	C
5	113.2	C	106.8	C	107.1	C	109.6	C	105.8	C	110.9	C	104.8	C
6	159.1	C	161.7	C	154.4	C	162.9	C	160.1	C	161.4	C	160.4	C
1′	68.7	CH	51.7	CH	76.7	CH	71.6	CH	37.8	CH$_2$	33.1	CH$_2$	33.6	CH$_2$
2′	39.4	CH$_2$	58.7	CH	81.7	CH	208.7	C	207.0	C	73.4	CH	208.5	C
3′	19.5	CH$_2$	21.8	CH$_2$	28.1	CH$_2$	30.8	CH$_2$	35.6	CH$_2$	31.1	CH$_2$	72.7	CH
4′	14.0	CH$_3$	10.4	CH$_3$	8.9	CH$_3$	7.9	CH$_3$	8.0	CH$_3$	10.7	CH$_3$	20.2	CH$_3$
4-OCH$_3$	56.3	CH$_3$	56.2	CH$_3$	56.9	CH$_3$	56.4	CH$_3$	56.4	CH$_3$	57.1	CH$_3$	56.5	CH$_3$
6-CH$_3$	17.9	CH$_3$	18.2	CH$_3$	17.8	CH$_3$	17.7	CH$_3$	17.6	CH$_3$	17.9	CH$_3$	17.7	CH$_3$

For solvents and magnetic field used for each compound, see the Materials and Methods section

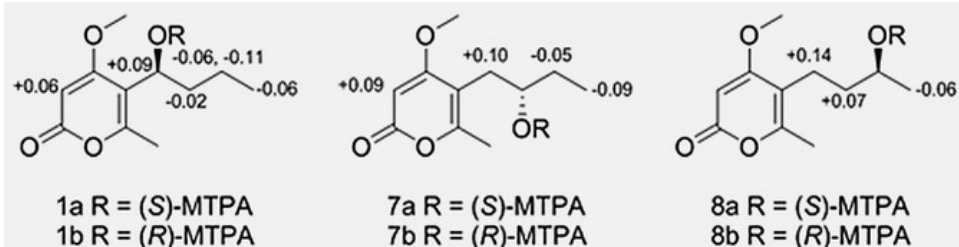**Figure 3.** $\Delta\delta_H$ values [$\Delta\delta$ (in ppm) $= \delta S - \delta R$] obtained for compounds **1**, **7**, and **8**.

Compound **2** was obtained as a colorless solid. The molecular formula was $C_{11}H_{14}O_4$ based on the HRESIMS data (*m/z* 211.0955), indicating five degrees of unsaturation. The 1D-NMR spectra of **2** were similar to those of **1**, except for the chemical shift of the proton and carbon signals attributed to the oxymethine at C-1′ in **1** (δ_H/δ_C 4.63/68.7), which were both relatively more shielded in **2** (δ_H/δ_C 3.71/51.7). Additionally, the replacement of a methylene group in **1** for an oxymethine group (δ_H/δ_C 3.10/58.7) in **2**, as well as the increase in the unsaturation number, indicated **2** as 1′,2′-epoxi-delitpyrone A (**2**). Key HMBC correlations ([Fig. 4]) confirmed the structure of **2**. The spatial orientation of the substituent at position 1′ was considered to be the same as in compound **1** based on the specific rotation ([α]$_D$ ^{27} $= -5$) and biogenetic considerations. The coupling constant ($J_{H-1'/H-2'} = 4.0$ Hz) did not permit a clear consideration of the orientation across the epoxide [30]. However, the isolation from this strain of the *E* oriented putative biosynthetic precursor of **2** (data not shown), as well as other analogues, supported the *trans* disposition of the substituents in the oxirane. Thus, the absolute configuration of **2** was presumed to be 1′R,2′R. While the absolute configuration at C-1′ in **1** is *S*, it became *R* in **2**, based on the Cahn-Ingold-Prelog rules.
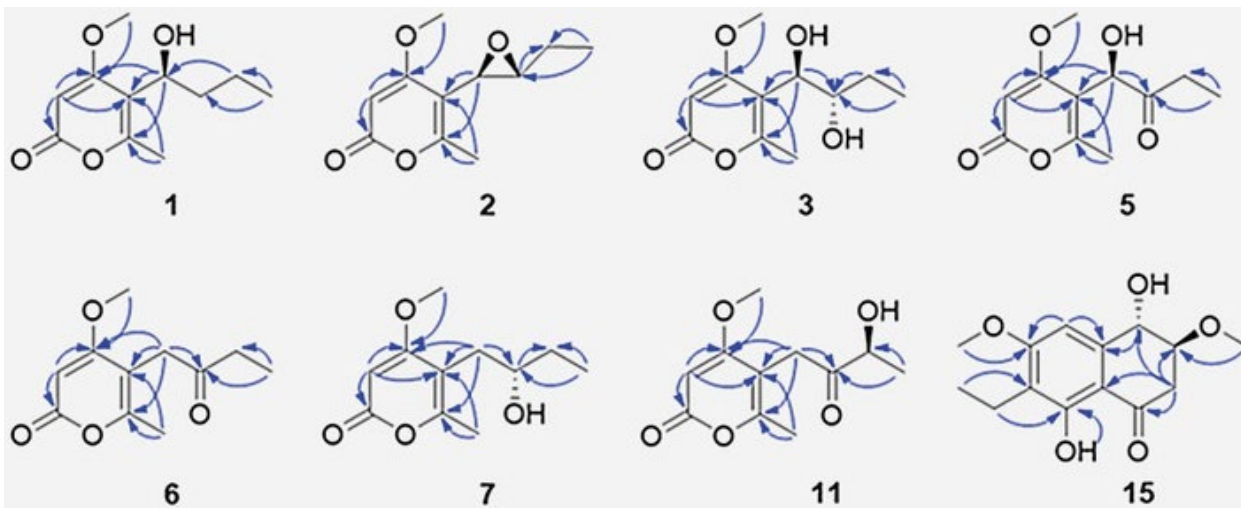
Figure 4. Key HMBC correlations of compounds **1**–**3**, **5**–**7**, **11**, and **15**.

Compound **3** (delitpyrone B) was isolated as a colorless solid, and its molecular formula was $C_{11}H_{16}O_5$ based on the HRESIMS data (*m/z* 229.1068). The NMR data for **3** resembled those for 1′,2′-epoxi-delitpyrone A (**2**). Key differences were the deshielding of the methine groups at C-1′ and C-2′ (δ_H/δ_C 5.15/76.7 and 4.52/81.7, respectively) ([Tables 1] and [2]), indicating the opening of the epoxide moiety by the nucleophilic substitution of water, yielding the diol

congener of **2**. HMBC correlations ([Fig. 4]) further confirmed the structure of **3**. The absolute configuration of compound **3** was proposed as 1′*R* and 2′*S* based on biogenic considerations.

Delitpyrone C (**4**) was isolated as a colorless solid, and its molecular formula was $C_{11}H_{14}O_4$ according to the HRESIMS data at *m/z* 211.0962, indicating five degrees of unsaturation. The ^{1}H-NMR for **4** was quite different than those recorded for **1**–**3**; for example, the characteristic methyl signal at $\delta_H \sim 2.3$ ppm (6-CH$_3$) was replaced by two vinylic protons at δ_H 4.81 (d, *J* = 1.9) and 5.07 (d, *J* = 1.9). Additionally, comparison of the ^{1}H-NMR data of **4** with that of **3** indicated the replacement of the oxymethine group at C-1′ with a vinylic proton δ_H 6.49 (d, *J* = 9.3) ([Table 3]). Altogether, this information indicated **4** as the dehydration product of **3**. Unfortunately, the 2D-NMR data for compound **4** were not collected due to the instability of the compound and the paucity of the sample. Interestingly, this compound was recently proposed as an intermediate in the biosynthesis of delitschiapyrone A, a pyrone-naphthalenone adduct isolated from the leaf-associated fungus *Delitschia* sp. FL1581 [12]. The isolation of **4** from a related species both supports the biosynthetic proposal [12] and suggests the conservation of biosynthetic machinery within this genus.

Table 3. NMR spectroscopic data for compound **4** (500 and 125 MHz, ^{1}H and ^{13}C, respectively), recorded in acetone-*d*$_6$.

Position	δ_C,	type	δ_H, multiplicity (*J* = Hz)
2	162.2	C	
3	78.7	CH	5.36, *s*
4	167.0	C	
5	123.5	C	
6	150.2	C	
1′	139.8	CH	6.49, *d* (9.3)
2′	69.3	CH	4.48, *m*
3′	31.2	CH$_2$	1.60, *m*
			1.67, *m*
4′	10.0	CH$_3$	0.99, *t* (7.4)
4-OCH$_3$	57.1	CH$_3$	3.92, *s*
6-CH$_{2a}$	90.6	CH$_2$	4.81, *d* (1.9)
6-CH$_{2b}$			5.07, *d* (1.9)

Compound **5** (2′-oxodelitpyrone A), the 2′-oxo analogue of delitpyrone A, was obtained as a colorless solid. The molecular formula was $C_{11}H_{14}O_5$ according to the HRESIMS data (*m/z* 227.0916). Analysis of the ^{1}H- and ^{13}C-NMR data ([Tables 1] and [2]) indicated that **5** shares the same core as **1**, with slight modifications in the side chain. The main difference was the replacement of the methylene group at the C-2′ position in **1** by a carbonyl group (δ_C 208.7) in **5**. The structure of **5** was confirmed through the analysis of the HMBC spectrum ([Fig. 4]). The spatial orientation of the hydroxy group in **5** was presumed to be in a *β* orientation by comparison of its specific rotation ($[\alpha]_D^{27} = -38$) with that recorded for **1**. However, the absolute configuration at C-1′ was assigned as *R*.

Delitpyrone D (**6**) was isolated as a colorless solid, and its molecular formula was $C_{11}H_{14}O_4$ according to the HRESIMS data (*m/z* 211.0967). The ^{1}H and ^{13}C-NMR data ([Tables 1] and [2])

were found to be similar with those of **5**, with a difference observed in the chemical shift attributed to C-1′. Briefly, the oxymethine group in **5** (δ_H/δ_C 4.98/71.6) was replaced by a methylene group in **6** (δ_H/δ_C 3.42/37.8). The splitting pattern of H_3-4′ (*t*) and H_2-3′ (*q*), as well as key HMBC correlations from H_2-1′and H_2-3′ to a ketone carbonyl group at C-2′ ([Fig. 4]), confirmed the structure of **6** as 1′-dehydroxy-2′-oxodelitpyrone A.

Compounds **7** and **8** (a known compound) were isolated as structural isomers sharing the molecular formula $C_{11}H_{16}O_4$, as determined by the HRESIMS data (*m/z* 213.1122 and 213.1121, respectively), with an index of hydrogen deficiency of four. The ^{1}H- and ^{13}C-NMR data for both compounds were similar to each other. In the case of **7**, signals for two methine groups, one vinylic proton (δ_H/δ_C 5.58/88.3, s for H-3/C-3), one oxymethine (δ_H/δ_C 3.55/73.4, C-2′), two methylene [(δ_H/δ_C 2.41/2.58/33.1 for H-1′a/H-1′b/C-1′) and (δ_H/δ_C 1.46/1.53/31.1 for H-3′a/H-3′b/C-3′)], and one methyl group (δ_H/δ_C 0.98/10.7, t, *J* = 7.4 Hz for H_3-4′/C-4′) were observed. Inspection of the splitting patterns in the ^{1}H-NMR spectra, together with HMBC correlations, established the structure of **7** as 5-(2-hydroxybutyl)-4-methoxy-6-methyl-2*H*-pyran-2-one, which was assigned the trivial name delitpyrone E. The absolute configurations at the chiral center in **7** (C-2′) was established as *S* via the modified Mosher's ester method ([Fig. 3]).

Compound **11** was isolated as a colorless solid, and its molecular formula was $C_{11}H_{14}O_5$ on the basis of the HRESIMS (*m/z* 227.0914), indicating five degrees of unsaturation. The 1D-NMR spectra were similar with those of **6**, with the exception of the signals attributed to protons and carbons at positions 3′ and 4′. Thus, the triplet and quartet in **6** (δ_H/δ_C 2.50/35.6, q, *J* = 7.3 Hz for H-3′/C-3′; 1.09/8.0, t, *J* = 7.3 Hz for H_3-4′/C-4′) were replaced by a doublet of quartets for an oxymethine and a methyl doublet in **11** (δ_H/δ_C 4.38/72.7, dq, *J* = 6.9, 5.0 Hz for H-3′/C-3′; 1.47/20.2, d, *J* = 7.1 Hz for H_3-4′/C-4′). Thus, **11** was determined to be 3′-hydroxydelitpyrone D, and its structure was confirmed by analysis of the HMBC spectrum ([Fig. 4]). The absolute configuration at C-3′ was presumed to be *S* based on biogenic considerations. The biosynthesis for compounds **1**–**11** is proposed (**Fig. 56S**, Supporting Information).

Compound **15** was isolated as a yellow solid, and its molecular formula was determined as $C_{14}H_{18}O_5$ by HRESIMS analysis (*m/z* 267.1224). The 1D- and 2D-NMR data for this compound suggested structural similarity with the known compound 6-ethyl-2,7-dimethoxyjuglone (**14**) [31],[32]. The key differences were the replacement of one sp^2 methine in **14** by a shielded methylene group at δ_H/δ_C (2.56; 3.15/40.9, dd, *J* = 16.8, 10.5 Hz; dd, *J* = 16.8, 4.4 Hz for H-3a/H-3b/C-3) in **15**, as well as the ^{13}C signals at C-4 and C-1 that were shielded from δ_C 179.8 to 72.1, and deshielded from δ_C 190.9 to 199.4, respectively, supporting the reduction of the *p*-naphthoquinone in **14** to a dihydronaphthalen-1(2*H*)-one moiety in **15** ([Table 4]). Inspection of the splitting patterns of signals, together with HMBC correlations ([Fig. 4]), established the structure of **15** as 7-ethyl-4,8-dihydroxy-3,6-dimethoxy-3,4-dihydronaphthalen-1(2*H*)-one. The relative configurations at positions C-3 and C-4 were established based on the analysis of coupling constant values and by comparison of the ^{1}H-NMR data collected for **15** with that reported for (3*S*,4*S*)-3,4,8-trihydroxy-3,4-dihydro-1(2*H*)-naphthalenone [33]. Briefly, a *trans*-pseudoaxial orientation between H-3 and H-4 was evident by the coupling constant $^3J_{H\text{-}3\text{-}H\text{-}4}$ = 8.7 Hz, placing the hydroxy and methoxy substituents in an *anti*-orientation. Therefore, compound **15** was characterized as 3*S**,4*S**-7-ethyl-4,8-dihydroxy-3,6-dimethoxy-3,4-dihydronaphthalen-1(2*H*)-one.

Table 4. NMR data for compound **15** (700 and 175 MHz, ^{1}H and ^{13}C, respectively), recorded in CDCl$_3$.

Position	δ_C	type	δ_H, multiplicity (J = Hz)
1	199.4	C	
2	40.9	CH$_2$	2.56, *dd* (16.8, 10.5)
			3.15, *dd* (16.8, 4.4)
3	80.4	CH	3.60, *ddd* (10.6, 8.7, 4.4)
4	72.1	CH	4.71, *dd* (8.8, 2.1)
4a	142.6*	C	
5	100.3	CH	6.80, *s*
6	164.3	C	
7	118.8	C	
8	161.8	C	
8a	110.1	C	
1′	15.7	CH$_2$	2.65, *q* (7.5)
2′	13.3	CH$_3$	1.08, *t* (7.5)
3-OCH$_3$	57.2	CH$_3$	3.49, *s*
6-OCH$_3$	56.0	CH$_3$	3.94, *s*
4-OH			2.90, *s*
8-OH			12.62, *s*

* Signal obtained from HMBC spectrum

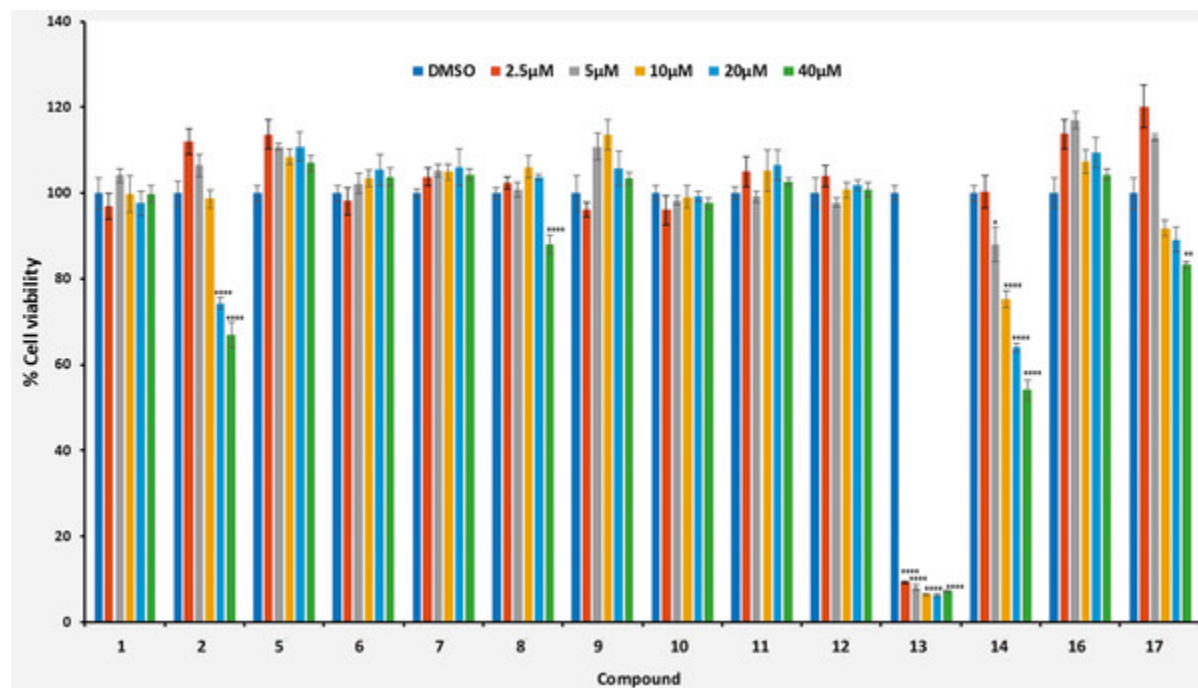**Figure 5.** Cytotoxic activity of compounds **1, 2, 5–14, 16**, and **17** against the African American prostate cancer cell line E006AA-hT. The percentage viability was calculated by comparing the absorbance of control and treated cells. Data represent the mean ± SE of five replicates; *p < 0.05, **p < 0.01, ****p < 0.0001, significant when compared to control.

The antiproliferative activities of compounds **1, 2, 5–14, 16**, and **17** were evaluated against the African American prostate cancer cell line (E006AA-hT) under hypoxic conditions ([Fig. 5]). Of

these, sporidesmin A (**13**) strongly inhibited the viability of the E006AA-hT cells in a concentration-dependent manner and was effective even at the lowest concentration tested, i.e., 2.5 µM (**Fig. 2S**, Supporting Information). Compounds **2** and 6-ethyl-2,7-dimethoxyjuglone (**14**) also showed moderate growth inhibitory activity, especially at the highest concentration of 40 µM ([Fig. 5]).

In summary, the construction of a peak library derived from freshwater aquatic fungi ([Fig. 1] and **Fig. 58S**, Supporting Information), followed by the chemical study of the active extract obtained from fungal strain G858 (*Delitschia* sp.), led to the identification of eight new α-pyrone derivatives (**1**–**7**, and **11**), as well as the new 3*S**,4*S**-7-ethyl-4,8-dihydroxy-3,6-dimethoxy-3,4-dihydronaphthalen-1(*2H*)-one (**15**). The cytotoxicity of compounds **1, 2, 5**–**14, 16**, and **17** was evaluated against an African American prostate cancer cell line (E006AA-hT), where **2, 13**, and **14** showed activity. These results highlight the potential of fungi from underexplored environments as a source of new chemical entities, contributing to the expansion of the chemical space of natural products.

Materials and Methods

General experimental procedures

Optical rotation and UV experiments were conducted using a Rudolph Research Autopol III polarimeter (Rudolph Research Analytical) and a Varian Cary 100 Bio UV-vis spectrophotometer (Varian Inc.). NMR data were obtained using either a JOEL ECA-500 NMR spectrometer operating at 500 MHz for ^{1}H and 125 MHz for ^{13}C (JOEL Ltd.) or an Agilent 700 MHz NMR spectrometer equipped with a cryoprobe, operating at 700 MHz for ^{1}H and 175 MHz for ^{13}C (Agilent Technologies). HRESIMS data were collected with a Thermo QExactive Plus mass spectrometer coupled with an electrospray ionization source (Thermo Fisher Scientific). The purity of the compounds (> 95%) was assessed by ^{1}H-NMR (see Supporting Information) and using a Waters Acquity UPLC system paired with an Acquity BEH C$_{18}$ column (1.7 µm; 50 mm × 2.1 mm) (Waters Corp.) and analyzed using the software XCalibur. Gemini-NX C$_{18}$ analytical (5 µm; 250 × 4.6 mm), semipreparative (5 µm; 250 × 10.0 mm), preparative (5 µm; 250 × 21.2 mm), Luna PFP semipreparative (5 µm; 250 × 10.0 mm) and preparative (5 µm; 250 × 21.2 mm) columns (all from Phenomenex) along with Waters Atlantis T3 C$_{18}$ semipreparative (5 µm; 250 × 10.0 mm) and preparative (5 µm; 250 × 19.0 mm) columns were used for chromatographic separations. A Varian ProStar HPLC system equipped with ProStar 210 pumps, a ProStar 335 photodiode array detector, and Galaxie Chromatography Workstation software (version 1.9.3.2, Varian Inc.) was used for data collection and analysis. Flash chromatography was conducted on a Teledyne Isco CombiFlash Rf 200 system using RediSep RF Gold HP silica columns (both from Teledyne Isco) that was coupled with UV and evaporative light-scattering detectors. All other reagents and solvents were obtained from Fisher Scientific.

Fungal strain isolation and identification

Specimen JF16003 was collected in Ariége, Rimont, France on submerged wood in LeBaup stream (September 2015) (**Fig. 58S**, Supporting Information) from which strain G858 was

isolated. Based on micromorphological examination of the fruiting bodies obtained from the incubated wood, the fungus was identified as *Delitschia* sp. (**Fig. 3S**, Supporting Information). This fungus develops on long-time submerged wood as a dense greenish black sterile subiculum, and ascomata occur when the stream dries out or when the wood is washed out on the banks. In addition, the partial large subunit (LSU; 28S) rDNA region was sequenced to corroborate morphological observations, since the 28S ribosomal gene region for most previously described *Delitschia* sp. is available in GenBank for phylogenetic comparison. The partial LSU region was amplified using primer combination LROR and LR6 [34],[35] and Sanger sequenced using primers LROR, LR3, and LR6. For phylogenetic analysis, all available *Delitschia* sp. sequences from GenBank were aligned using a previously published LSU alignment of members of the Pleosporomycetidae, Dothideomycetes [36]; these included reports of *Delitschia* sp. from which fungal metabolites have been isolated [12],[13],[26]. Protocols for DNA extraction, PCR, Sanger sequencing, and phylogenetic analysis have been reviewed [37]. Results of the Maximum Likelihood (ML) analysis showed that strain G858 was nested within the family Delitschiaceae, Pleosporales, Dothideomycetes, Ascomycota with 100% ML bootstrap and was a sister to *Delitschia* sp. (FL1581) [12] with high bootstrap support (**Fig. 3S**, Supporting Information). *Delitschia* sp. have been reported from herbivore dung [12],[38],[39] and submerged wood in freshwater [26],[40]. This study provides molecular evidence that *Delitschia* is not restricted to a coprophilous lifestyle but can also be lignicolous (**Fig. 4S**, Supporting Information). The partial LSU sequences were deposited in GenBank (MF684774, MF684775).

Fermentation, extraction, and isolation

A fresh culture of fungal strain G858 was grown in a petri dish containing potato dextrose agar (PDA; Difco) with an autoclaved piece of balsa wood. Once sufficient mycelial growth was observed on the PDA plates, a small agar plug with fungal mycelium was cut out from the leading edge of the colony and transferred aseptically to eight 10-mL liquid YESD (2% soy peptone, 2% dextrose, and 1% yeast extract) seed cultures. The cultures were shaken at room temperature at 125 rpm for 14 days. Afterwards, the seed cultures were used to inoculate eight 250-mL Erlenmeyer flasks with solid media (rice), prepared by autoclaving 10 g of rice with 20 mL of distilled H_2O; the flasks were incubated at room temperature for 28 days [8],[9].

A total of 60 mL of 1:1 MeOH-CHCl$_3$ was added to each of the flasks followed by chopping into small pieces with a spatula. The samples were shaken overnight (~ 16 h) using a rotary shaker at ~ 125 rpm at room temperature, filtered under vacuum, and the remaining solid portions were washed with small volumes of MeOH. The filtrates were combined, and 300 mL of both CHCl$_3$ and H_2O were added. This biphasic solution was stirred for 30 min and transferred to a separatory funnel in which a precipitate was collected prior to the organic layer being drawn off; both the organic phase and the precipitate were evaporated to dryness in vacuum. The organic extract was partitioned between 300 mL of 1:1 MeOH-CH$_3$CN and 300 mL of hexanes. The MeOH-CH$_3$CN layer was evaporated under reduced pressure to dryness [8],[21]. The defatted extract (~ 559 mg) was dissolved in CHCl$_3$, then adsorbed onto Celite 545. The sample was fractionated by flash chromatography via a 24 g RediSep Rf Gold HP silica column using a gradient solvent system of hexane-CHCl$_3$-MeOH at a 35 mL/min flow rate and 25.7 column volumes over 24.7 min to afford nine fractions (F1–F9). Fraction 3 (63.6 mg) was subjected to

preparative HPLC using a gradient system of 50:50 to 80:20 CH_3CN-H_2O (0.1% formic acid) over 30 min at a flow rate of 21.20 mL/min and a Gemini column to yield compound **14** (4.6 mg, t_R 18.0 min). Fraction 4 (73.8 mg) was subjected to preparative HPLC using a gradient system of 20:80 to 100:0 CH_3CN-H_2O (0.1% formic acid) over 30 min at a flow rate of 20.00 mL/min and a Gemini column to yield 10 subfractions (F4$_I$-F4$_X$). Subfractions F4$_I$ and F4$_{IV}$ afforded compounds **2** (1.3 mg) and **15** (2.0 mg), respectively. Fraction 5 (9.6 mg) was subjected to semipreparative HPLC using a gradient system of 40:60 to 70:30 CH_3CN-H_2O (0.1% formic acid) over 30 min at a flow rate of 4.60 mL/min and a Gemini column to yield 6 subfractions, where subfraction 3 yielded compound **13** (2.5 mg, t_R 13.7 min). Fraction 6 (136.7 mg) was subjected to preparative HPLC using a gradient system of 10:90 to 50:50 CH_3CN-H_2O (0.1% formic acid) over 30 min at a flow rate of 21.20 mL/min and a Gemini column to yield 18 subfractions (F6$_I$-F6$_{XVIII}$). Subfractions F6$_I$, F6$_{IV}$, F6$_{VI}$, F6$_{VII}$, and F6$_{XII}$ afforded compounds **5** (10.3 mg, t_R 10.1 min), **9** (1.0 mg, t_R 14.9 min), **6** (8.7 mg, t_R 16.0 min), **1** (11.0 mg, t_R 17.2 min), and **12** (0.9 mg, t_R 22.1 min), respectively. Subfraction F6$_V$ (17.3 mg) was further purified with preparative HPLC using an isocratic system 25:75 CH_3CN-H_2O (0.1% formic acid) over 20 min at a flow rate of 21.20 mL/min and a Luna PFP column to yield 6 subfractions, in which subfraction 1 afforded compound **10** (0.4 mg, t_R 7.5 min). Subfraction F6$_X$ (6.8 mg) was further purified with semipreparative HPLC using a gradient system of 35:65 to 45:55 CH_3CN-H_2O (0.1% formic acid) over 30 min at a flow rate of 4.60 mL/min and a Gemini column to yield 4 subfractions (F6$_{X1}$-F6$_{X4}$), where F6$_{X2}$, and F6$_{X3}$ afforded compounds **4** (1.6 mg, t_R 9.8 min) and **3** (0.8 mg, t_R 10.3 min), respectively. Fraction 7 (242.0 mg) was subjected to two different purification methods using preparative HPLC. Part of fraction 7 (100.0 mg) was subjected to preparative HPLC using a gradient system of 20:80 to 100:0 CH_3CN-H_2O (0.1% formic acid) over 30 min at a flow rate of 17.00 mL/min and an Atlantis T3 column to yield 9 subfractions (F7$_{A–I}$-F7$_{A-IX}$). Subfractions F7$_{A-II}$ and F7$_{A-III}$ afforded compounds **8** (3.7 mg, t_R 8.0 min) and **7** (9.0 mg, t_R 9.4 min), respectively. Part of fraction 7 (100.0 mg) was subjected to preparative HPLC using a gradient system of 10:90 to 50:50 CH_3CN-H_2O (0.1% formic acid) over 30 min at a flow rate of 21.20 mL/min and a Luna PFP column to yield 18 subfractions, where subfraction 4 afforded compound **11** (0.9 mg, t_R 10.6 min). The precipitate obtained from the $CHCl_3$-H_2O partition (80.0 mg) was subjected to preparative HPLC using a gradient system of 60:40 to 90:10 CH_3CN-H_2O (0.1% formic acid) over 30 min at a flow rate of 21.20 mL/min and a Gemini column to yield 8 subfractions. Subfraction 2 yielded compound **17** (1.3 mg), and subfractions 4–6 afforded compound **16** (47.1 mg). Compounds **3, 7, 8**, and **15** were further purified by analytical and semipreparative HPLC to generate materials of a higher purity, while all other isolated compounds were at a suitable purity for biological evaluation. Various columns and gradients, including isocratic, were used with a mobile phase of CH_3CN-H_2O (0.1% formic acid) to yield compounds **3** (0.1 mg), **7** (2.3 mg), **8** (1.3 mg), and **15** (0.4 mg).

Delitpyrone A (**1**): Colorless solid; $[\alpha]_D^{27} = -15$ (*c* 0.1, MeOH); UV (MeOH) λ_{max} (log ε) 209 (4.17), 284 (3.82) nm; ^{1}H-NMR (CDCl$_3$, 700 MHz) and ^{13}C-NMR (CDCl$_3$, 175 MHz), see [Tables 1] and [2]; HRESIMS *m/z* 213.1125 (calcd. for $C_{11}H_{17}O_4$, 213.1121).

1′,2′-Epoxi-delitpyrone A (**2**): Colorless solid; $[\alpha]_D^{26} = -5$ (*c* 0.04, MeOH); UV (MeOH) λ_{max} (log ε) 208 (3.78), 284 (3.22) nm; ^{1}H-NMR (CDCl$_3$, 500 MHz) and ^{13}C-NMR

(CDCl$_3$, 125 MHz), see [Tables 1] and [2]; HRESIMS *m/z* 211.0955 (calcd. for C$_{11}$H$_{15}$O$_4$, 211.0965).

Delitpyrone B (**3**): Colorless solid; ^{1}H-NMR (CDCl$_3$, 700 MHz) and ^{13}C-NMR (CDCl$_3$, 175 MHz), see [Tables 1] and [2]; HRESIMS *m/z* 229.1068 (calcd. for C$_{11}$H$_{17}$O$_5$, 229.1070).

Delitpyrone C (**4**): Colorless solid; ^{1}H-NMR (acetone-*d*$_6$, 500 MHz) and ^{13}C-NMR (acetone-*d*$_6$, 125 MHz), see [Table 3]; HRESIMS *m/z* 211.0962 (calcd. for C$_{11}$H$_{15}$O$_4$, 211.0965).

2′-Oxodelitpyrone A (**5**): Colorless solid; $[\alpha]_D{}^{27} = -38$ (*c* 0.1, MeOH); UV (MeOH) λ_{max} (log ε) 208 (4.11), 276 (3.74) nm; ^{1}H-NMR (CDCl$_3$, 500 MHz) and ^{13}C-NMR (CDCl$_3$, 125 MHz), see [Tables 1] and [2]; HRESIMS *m/z* 227.0916 (calcd. for C$_{11}$H$_{15}$O$_5$, 227.0914).

Delitpyrone D (**6**): Colorless solid; UV (MeOH) λ_{max} (log ε) 208 (4.30), 283 (3.94) nm; ^{1}H-NMR (CDCl$_3$, 500 MHz) and ^{13}C-NMR (CDCl$_3$, 125 MHz), see [Tables 1] and [2]; HRESIMS *m/z* 211.0967 (calcd. for C$_{11}$H$_{15}$O$_4$, 211.0965).

Delitpyrone E (**7**): Colorless solid; $[\alpha]_D{}^{27} = +17$ (*c* 0.13, MeOH); UV (MeOH) λ_{max} (log ε) 210 (3.92), 285 (3.65) nm; ^{1}H-NMR and ^{13}C-NMR (MeOH-*d*$_4$, 500 MHz), see [Tables 1] and [2]; HRESIMS *m/z* 213.1122 (calcd. for C$_{11}$H$_{17}$O$_4$, 213.1121).

5-(3-S-Hydroxybutyl)-4-methoxy-6-methyl-2H-pyran-2-one (**8**): Colorless solid; $[\alpha]_D{}^{27} = +7$ (*c* 0.09, MeOH); UV (MeOH) λ_{max} (log ε) 210 (3.73), 284 (3.41) nm; ^{1}H-NMR and ^{13}C-NMR (MeOH-*d*$_4$, 500 MHz), see Supporting Information; HRESIMS *m/z* 213.1121 (calcd. for C$_{11}$H$_{17}$O$_4$, 213.1121).

*4-Methoxy-6-methyl-5-(3-oxobutyl)-2*H*-pyran-2-one* (**9**): Colorless solid; UV (MeOH) λ_{max} (log ε) 207 (3.67), 281 (3.12) nm; ^{1}H-NMR (MeOH-*d*$_4$, 500 MHz) and ^{13}C-NMR (MeOH-*d*$_4$, 125 MHz), see Supporting Information; HRESIMS *m/z* 211.0968 (calcd. for C$_{11}$H$_{15}$O$_4$, 211.0965).

Pyrenocine I (**10**): Colorless solid; UV (MeOH) λ_{max} (log ε) 232 (3.75), 284 (3.41) nm; ^{1}H-NMR and ^{13}C-NMR (CDCl$_3$, 500 MHz), see Supporting Information; HRESIMS *m/z* 211.0965 (calcd. for C$_{11}$H$_{15}$O$_4$, 211.0965).

3′-Hydroxydelitpyrone D (**11**): Colorless solid; UV (MeOH) λ_{max} (log ε) 211 (3.53), 2863 (3.43) nm; ^{1}H-NMR and ^{13}C-NMR (CDCl$_3$, 500 MHz), see [Tables 1] and [2]; HRESIMS *m/z* 227.0914 (calcd. for C$_{11}$H$_{15}$O$_5$, 227.0914).

3S,4S*-7-Ethyl-4,8-dihydroxy-3,6-dimethoxy-3,4-dihydronaphthalen-1(2*H*)-one* (**15**): Yellow solid; ^{1}H-NMR and ^{13}C-NMR (CDCl$_3$, 700 MHz), see [Table 4]; HRESIMS *m/z* 267.1224 (calcd. for C$_{14}$H$_{19}$O$_5$, 267.1227).

Preparation of the (*R*)- and (*S*)-MTPA ester derivatives of compounds 1, 7, and 8

Independently, a total of 0.10 mg of compounds **1, 7**, and **8** were mixed with 400 μL of pyridine-*d* $_5$ and transferred into NMR tubes. The reactions were initiated with the addition of 4 μL of *S*-(+)-α-methoxy-α-(trifluoromethyl)phenylacetyl (MTPA) chloride into each NMR tube. The tubes were carefully shaken and then immediately monitored by ¹H-NMR at 5, 10, and 15 min increments, with the reactions being completed by 10 min, yielding the mono (*R*)-MTPA ester derivatives of **1, 7**, and **8** (**1b, 7b**, and **8b**, respectively). The (*S*)-MTPA ester derivatives of compounds **1, 7**, and **8** (**1a, 7a**, and **8a**, respectively) were prepared in an analogous similar fashion [9].

Cell viability assay

African American cancer cells (E006AA-hT) were obtained from Dr. Koochekpour (Roswell Park Memorial Institute). Cells were treated with **1, 2, 5−14, 16**, and **17** (2.5−40 μM, in DMSO) and cultured under hypoxia (1% O_2) for 48 h. An equal amount of DMSO was present in each treatment, including the control; the concentration of DMSO did not exceed 0.1% (v/v) in any treatment. Cell viability was measured using the MTT reagent, as detailed below. As a positive control, we used the HIF2α inhibitor TC-S7009, which in our other completed studies inhibited E006AA-hT cell viability with an IC_{50} value of ~ 20 μM; HIF2α inhibitors are important anticancer molecules [41]. TC-S7009 (≥ 99% purity) was procured from Tocris Bioscience (Avonmouth, Bristol).

For the MTT assay, 2000 E006AA-hT cells in 200 μL of media were dispensed in a 96-well plate on day 1, followed by exposure to **1, 2, 5−14, 16**, and **17** at concentrations of 2.5−40 μM on day 2, and then cultured under hypoxic conditions (1% oxygen concentration). After 48 h of hypoxia treatment, 20 μL of MTT (5 mg/mL PBS) were added to each well. The plates were further incubated for 2 h. Following completion of the incubation time, the medium was decanted, the formazan formed was dissolved in 200 μL of DMSO, and, after 10 min, absorbance was measured at 550 and 660 nm on a microplate reader.

References

1. Hawksworth DL, Lücking R. Fungal diversity revisited: 2.2 to 3.8 million species. Microbiol Spectr 2017; 5: 1-17

2. Choi J, Kim SH. A genome tree of life for the Fungi kingdom. Proc Natl Acad Sci U S A 2017; 114: 9391-9396

3. Shearer CA, Raja HA. Freshwater ascomycetes database. Available at: http://fungi.life.illinois.edu/ Accessed January 14, 2018

4. Cai L, Hu DM, Liu F, Hyde KD, Gareth-Jones E. The molecular Phylogeny of freshwater Sordariomycetes and Discomycetes. In: Jones EBG, Hyde KD, Pang KL. eds. Freshwater Fungi and fungal-like Organisms. Berlin: De Gruyter; 2014: 47-72

5. Wong MKM, Goh TK, Hodgkiss IJ, Hyde KD, Ranghoo VM, Tsui CKM, Ho WH, Wong WSW, Yuen TK. Role of fungi in freshwater ecosystems. Biodivers Conserv 1998; 7: 1187-1206

6. Hernández-Carlos B, Gamboa-Angulo MM. Metabolites from freshwater aquatic microalgae and fungi as potential natural pesticides. Phytochem Rev 2011; 10: 261-286

7. Shearer CA, Descals E, Kohlmeyer B, Kohlmeyer J, Marvanová L, Padgett D, Porter D, Raja HA, Schmit JP, Thorton HA. Fungal biodiversity in aquatic habitats. Biodivers Conserv 2007; 16: 49-67

8. Paguigan ND, Raja HA, Day CS, Oberlies NH. Acetophenone derivatives from a freshwater fungal isolate of recently described *Lindgomyces madisonensis* (G416). Phytochemistry 2016; 126: 59-65

9. El-Elimat T, Raja HA, Day CS, Chen WL, Swanson SM, Oberlies NH. Greensporones: resorcylic acid lactones from an aquatic *Halenospora* sp. J Nat Prod 2014; 77: 2088-2098

10. El-Elimat T, Raja HA, Figueroa M, Falkinham 3rd JO, Oberlies NH. Isochromenones, isobenzofuranone, and tetrahydronaphthalenes produced by *Paraphoma radicina*, a fungus isolated from a freshwater habitat. Phytochemistry 2014; 104: 114-120

11. Ainsworth GC. Ainsworth & Bisby's Dictionary of the Fungi. Wallingtonford, CT: Cabi; 2008

12. Luo JG, Wang XB, Xu YM, U'Ren JM, Arnold AE, Kong LY, Gunatilaka AAL. Delitschiapyrone A, a pyrone-naphthalenone adduct bearing a new pentacyclic ring system from the leaf-associated fungus *Delitschia* sp. FL1581. Org Lett 2014; 16: 5944-5947

13. Jayanetti DR, Li Y, Bartholomeusz GA, Bills GF, Gloer JB. Benzophenone and fimetarone derivatives from the coprophilous fungus *Delitschia confertaspora* . J Nat Prod 2017; 80: 707-712

14. Huang FW, Mosquera JM, Garofalo A, Oh C, Baco M, Amin-Mansour A, Rabasha B, Bahl S, Mullane SA, Robinson BD, Aldubayan S, Khani F, Karir B, Kim E, Chimene-Weiss J, Hofree M, Romanel A, Osborne JR, Kim JW, Azabdaftari G, Woloszynska-Read A, Sfanos K, De Marzo AM, Demichelis F, Gabriel S, Van Allen EM, Mesirov J, Tamayo P, Rubin MA, Powell IJ, Garraway LA. Exome sequencing of African-American prostate cancer reveals loss-of-function *ERF* mutations. Cancer Discov 2017; 7: 973-983

15. Panigrahi GK, Deep G. Exosomes-based biomarker discovery for diagnosis and prognosis of prostate cancer. Front Biosci (Landmark Ed) 2017; 22: 1682-1696

16. Deep G, Panigrahi GK. Hypoxia-induced signaling promotes prostate cancer progression: exosomes role as messenger of hypoxic response in tumor microenvironment. Crit Rev Oncog 2015; 20: 419-434

17. El-Elimat T, Figueroa M, Ehrmann BM, Cech NB, Pearce CJ, Oberlies NH. High-resolution MS, MS/MS, and UV database of fungal secondary metabolites as a dereplication protocol for bioactive natural products. J Nat Prod 2013; 76: 1709-1716

18. Paguigan ND, El-Elimat T, Kao D, Raja HA, Pearce CJ, Oberlies NH. Enhanced dereplication of fungal cultures via use of mass defect filtering. J Antibiot 2017; 70: 553-561

19. Karakashev SV, Reginato MJ. Progress toward overcoming hypoxia-induced resistance to solid tumor therapy. Cancer Manag Res 2015; 7: 253-264

20. Tredan O, Galmarini CM, Patel K, Tannock IF. Drug resistance and the solid tumor microenvironment. J Natl Cancer Inst 2007; 99: 1441-1454

21. Rivera-Chávez J, Raja HA, Graf TN, Burdette JE, Pearce CJ, Oberlies NH. Biosynthesis of fluorinated peptaibols using a site-directed building block incorporation approach. J Nat Prod 2017; 80: 1883-1892

22. Metwaly AM, Wanas AS, Radwan MM, Ross SA, ElSohly MA. New *α*-pyrone derivatives from the endophytic fungus *Embellisia* sp. Med Chem Res 2017; 26: 1796-1800

23. Metwaly AM, Fronczek FR, Ma G, Kadry HA, El-Hela AA, Mohammad AI, Cutler SJ, Ross SA. Antileukemic *α*-pyrone derivatives from the endophytic fungus *Alternaria phragmospora* . Tetrahedron Lett 2014; 55: 3478-3481

24. Hashida J, Niitsuma M, Iwatsuki M, Mori M, Ishiyama A, Namatame M, Nishihara-Tsukashima A, Nonaka K, Ui H, Masuma R, Otoguro K, Yamada H, Shiomi K, Ōmura S. Pyrenocine I, a new pyrenocine analog produced by *Paecilomyces* sp. FKI-3573. J Antibiot (Tokyo) 2010; 63: 559

25. Dingley JM, Done J, Taylor A, Russell DW. The production of sporidesmin and sporidesmolides by wild isolates of *Pithomyces chartarum* in surface and in submerged culture. Microbiology 1962; 29: 127-135

26. Sun R, Gao YX, Shen KZ, Xu YB, Wang CR, Liu HY, Dong JY. Antimicrobial metabolites from the aquatic fungus *Delitschia corticola* . Phytochem Lett 2011; 4: 101-105

27. Vijayakumar EKS, Roy K, Chatterjee S, Deshmukh SK, Ganguli BN, Fehlhaber HW, Kogler H. Arthrichitin. A new cell wall active metabolite from *Arthrinium phaeospermum* . J Org Chem 1996; 61: 6591-6593

28. Schlingmann G, Milne L, Williams DR, Carter GT. Cell wall active antifungal compounds produced by the marine fungus *Hypoxylon oceanicum* LL-15G256. II. Isolation and structure determination. J Antibiot (Tokyo) 1998; 51: 303-316

29. Hoye TR, Jeffrey CS, Shao F. Mosher ester analysis for the determination of absolute configuration of stereogenic (chiral) carbinol carbons. Nat Protocols 2007; 2: 2451-2458

30. Pavia DL, Lampman GM, Kriz GS, Vyvyan JA. Introduction to spectroscopy. 5th ed. Stamford, Connecticut: Cengage Learning; 2015: 359

31. Bentley R, Banach WJ, McInnes AG, Walter JA. 6-Ethyl-5-hydroxy-2,7-dimethoxy-1,4-naphthoquinone from *Hendersonula toruloidea*: A biosynthetic study using ^{13}C labels detected by nuclear magnetic resonance and ^{14}C tracers. Bioorg Chem 1981; 10: 399-411

32. Howe R, Moore RH. 6-ethyl-5-hydroxy-2,7-dimethoxynaphthoquinone, a metabolite of *Hendersonula toruloidea* Nattrass. Experientia 1969; 25: 474

33. Pittayakhajonwut P, Sohsomboon P, Dramae A, Suvannakad R, Lapanun S, Tantichareon M. Antimycobacterial substances from *Phaeosphaeria* sp. BCC8292. Planta Med 2008; 74: 281-286

34. Vilgalys R, Hester M. Rapid genetic identification and mapping of enzymatically amplified ribosomal DNA from several *Cryptococcus* species. J Bacteriol 1990; 172: 4238-4246

35. Rehner SA, Samuels GJ. Molecular systematics of the Hypocreales: a teleomorph gene phylogeny and the status of their anamorphs. Can J Bot 1995; 73: S816-S823

36. Mugambi G, Huhndorf S. Molecular phylogenetics of Pleosporales: Melanommataceae and Lophiostomataceae re-circumscribed (Pleosporomycetidae, Dothideomycetes, Ascomycota). Stud Mycol 2009; 64: 103-121

37. Raja HA, Miller AN, Pearce CJ, Oberlies NH. Fungal identification using molecular tools: a primer for the natural products research community. J Nat Prod 2017; 80: 756-770

38. Calaça F, Delpont M, Xavier-Santos S. *Delitschia gigaspora* var. pescanii: a new variety of coprophilous fungus from Brazil. Mycosphere 2015; 6: 122-126

39. Luck-Allen ER, Cain RF. Additions to the genus *Delitschia* . Can J Bot 1975; 53: 1827-1887

40. Hyde KD, Steinke TS. Two new species of *Delitschia* from submerged wood. Mycoscience 1996; 37: 99-102

41. Wallace EM, Rizzi JP, Han G, Wehn PM, Cao Z, Du X, Cheng T, Czerwinski RM, Dixon DD, Goggin BS, Grina JA, Halfmann MM, Maddie MA, Olive SR, Schlachter ST, Tan H, Wang

B, Wang K, Xie S, Xu R, Yang H, Josey JA. A small-molecule antagonist of HIF2α is efficacious in preclinical models of renal cell carcinoma. Cancer Res 2016; 76: 5491-5500